Id2-, RORγt-, and LTβR-independent initiation of lymphoid organogenesis in ocular immunity

Takahiro Nagatake,[1,5] Satoshi Fukuyama,[1] Dong-Young Kim,[1,6] Kaoru Goda,[1] Osamu Igarashi,[1] Shintaro Sato,[1] Tomonori Nochi,[1] Hiroshi Sagara,[2] Yoshifumi Yokota,[7] Anton M. Jetten,[8] Tsuneyasu Kaisho,[9] Shizuo Akira,[10] Hitomi Mimuro,[3] Chihiro Sasakawa,[3] Yoshinori Fukui,[11] Kohtaro Fujihashi,[12] Taishin Akiyama,[4] Jun-ichiro Inoue,[4] Josef M. Penninger,[13] Jun Kunisawa,[1,14] and Hiroshi Kiyono[1,5,12,14]

[1]Division of Mucosal Immunology, Department of Microbiology and Immunology, [2]Medical Proteomics Laboratory, [3]Division of Bacterial Infection, Department of Microbiology and Immunology, and [4]Division of Cellular and Molecular Biology, The Institute of Medical Science, The University of Tokyo, Minato-ku, Tokyo 108-8639, Japan
[5]Graduate School of Medicine and Faculty of Medicine, The University of Tokyo, Bunkyo-ku, Tokyo 113-0033, Japan
[6]Department of Otorhinolaryngology, Seoul National University College of Medicine, Chongno-gu, Seoul 110-744, Korea
[7]Department of Molecular Genetics, School of Medicine, University of Fukui, Eiheiji-cho, Yoshida-gun, Fukui 910-1193, Japan
[8]Cell Biology Section, Laboratory of Respiratory Biology, National Institute of Environmental Health Sciences, National Institutes of Health, Research Triangle Park, NC 27709
[9]Laboratory for Host Defense, Research Center for Allergy and Immunology, Institute of Physical and Chemical Research, Tsurumi-ku, Yokohama, Kanagawa 230-0045, Japan
[10]Laboratory of Host Defense, World Premier International Research Center–Immunology Frontier Research Center, Osaka University, Suita, Osaka 565-0871, Japan
[11]Division of Immunogenetics, Department of Immunobiology and Neuroscience, Medical Institute of Bioregulation, Kyushu University, Fukuoka 812-8582, Japan
[12]Immunobiology Vaccine Center, Department of Pediatric Dentistry, The University of Alabama at Birmingham, Birmingham, AL 35294
[13]Institute of Molecular Biotechnology of the Austrian Academy of Sciences, 1030 Vienna, Austria
[14]Graduate School of Frontier Sciences, The University of Tokyo, Kashiwa, Chiba 277-8561, Japan

CORRESPONDENCE
Hiroshi Kiyono:
kiyono@ims.u-tokyo.ac.jp

The eye is protected by the ocular immunosurveillance system. We show that tear duct–associated lymphoid tissue (TALT) is located in the mouse lacrimal sac and shares immunological characteristics with mucosa-associated lymphoid tissues (MALTs), including the presence of M cells and immunocompetent cells for antigen uptake and subsequent generation of mucosal immune responses against ocularly encountered antigens and bacteria such as *Pseudomonas aeruginosa*. Initiation of TALT genesis began postnatally; it occurred even in germ-free conditions and was independent of signaling through organogenesis regulators, including inhibitor of DNA binding/differentiation 2, retinoic acid–related orphan receptor γt, lymphotoxin (LT) α1β2–LTβR, and lymphoid chemokines (CCL19, CCL21, and CXCL13). Thus, TALT shares immunological features with MALT but has a distinct tissue genesis mechanism and plays a key role in ocular immunity.

Abbreviations used: AID, activation-induced cytidine deaminase; CALT, conjunctiva-associated lymphoid tissue; CT, cholera toxin; FAE, follicle-associated epithelium; FDC, follicular DC; GC, germinal center; HE, hematoxylin and eosin; HEV, high endothelial venule; Id2, inhibitor of DNA binding/differentiation 2; ILF, isolated lymphoid follicle; LT, lymphotoxin; LTi, lymphoid tissue inducer; MAdCAM-1, mucosal addressin cell adhesion molecule 1; MALT, mucosa-associated lymphoid tissue; NALT, nasopharynx-associated lymphoid tissue; NIK, NF-κB–inducing kinase; NP, nasal passage; pLN, peripheral LN; PNA, peanut agglutinin; PNAd, pLN addressin; PP, Peyer's patch; ROR, retinoic acid–related orphan receptor; TALT, tear duct–associated lymphoid tissue; TLR, Toll-like receptor; TRAF, TNF receptor–associated factor; TRANCE, TNF-related activation-induced cytokine; UEA, *Ulex europaeus* agglutinin; VCAM-1, vascular cell adhesion molecule 1.

Mucosa-associated lymphoid tissues (MALTs), including nasopharynx-associated lymphoid tissue (NALT) and Peyer's patches (PPs), are gateways for the uptake of inhaled and ingested antigens from the lumen of the aerodigestive tract, and are considered to be the sites of induction of mucosal immune responses (Mestecky et al., 2003; Kiyono and Fukuyama, 2004). The ocular surface leading to the lacrimal sac and nasolacrimal duct also forms an interface with the outside environment. In fact, it has been proposed that conjunctiva-associated lymphoid tissue (CALT), together with tear duct–associated lymphoid tissue (TALT), organizes eye-associated lymphoid tissue to create mucosal surveillance and a barrier in the eye

The Rockefeller University Press $30.00
J. Exp. Med. Vol. 206 No. 11 2351-2364
www.jem.org/cgi/doi/10.1084/jem.20091436

region of humans (Knop and Knop, 2000, 2001). Past investigations have focused on the identification and characterization of CALT (Gomes et al., 1997; Chodosh et al., 1998; Knop and Knop, 2000, 2005; Giuliano et al., 2002; Cain and Phillips, 2008). Mice and rats do not possess CALT, whereas other mammals (e.g., cats, dogs, and humans) do develop CALT (Chodosh et al., 1998). Rat conjunctivae, lacrimal glands, and harderian glands contain immunocompetent cells (e.g., $CD4^+$ and $CD8^+$ cells; Gomes et al., 1997); however, the immunocompetent cells do not form any organized microarchitecture at the conjunctiva and are thus diffusely located. Tears contain cytokines (e.g., IL-1, IL-4, IL-6, and TGF-β), antimicrobial peptides (e.g., lactoferrin and defensin), and secretory IgA; these secretions are an important arm of mucosal innate and acquired immunity, and respond to antigens that contact and invade the eye (Allansmith et al., 1985; Kijlstra, 1990; Gupta et al., 1996; Haynes et al., 1998; Nakamura et al., 1998; Uchio et al., 2000). Tear flow does not just provide mucosal protection at the ocular surface; it also connects the ocular surface with the nasal cavity via the tear duct, suggesting that tear flow is integral to regulating the homeostasis of the oculonasal mucosal barrier. On the other hand, the eye is considered to be an immune-privileged site, because the microenvironment of the eye is regulated by several complex aspects of the immune system (Stein-Streilein and Taylor, 2007). However, little information is currently available about the immunological nature of the eye-associated lymphoid tissue system—particularly the regulation of the tissue genesis of TALT and its immunological functions—despite the fact that TALT develops in humans (Knop and Knop, 2000, 2001).

Organogenesis of secondary lymphoid tissues, such as PPs and peripheral LNs (pLNs), is dependent on inflammatory cytokines, the release of which is mediated by lymphotoxin (LT) β receptor (LTβR) signals during the embryonic period (Mebius, 2003). The basis of LT-mediated lymphoid organ development at a molecular level was first shown in genetically manipulated *Lt*$\alpha^{-/-}$ mice, which lack PPs and pLNs (De Togni et al., 1994). Injection of an agonistic LTβR antibody into *Lt*$\alpha^{-/-}$ mice during a limited period in embryogenesis regenerates pLNs (Rennert et al., 1998). The physiological ligand of LTβR is a membrane-bound form of LTα1β2 produced by $CD3^-CD4^+CD45^+$ lymphoid tissue inducer (LTi) cells expressing IL-7Rα (Mebius et al., 1997). IL-7Rα–mediated signals trigger LTi cells to produce LTα1β2, and *Il-7r*$\alpha^{-/-}$ mice do not form PPs (Adachi et al., 1998b; Honda et al., 2001). In addition, deficiency of either inhibitor of DNA binding/differentiation 2 (Id2) or the retinoic acid–related orphan receptor (ROR) γt gene results in a lack of PPs and pLNs because the differentiation of $CD3^-CD4^+CD45^+$ LTi cells is impaired (Yokota et al., 1999; Sun et al., 2000; Eberl et al., 2004). These facts indicate the importance of inflammation-related cytokines, as well as Id2- and RORγt-subordinated $CD3^-CD4^+CD45^+$ LTi cells, in the organogenesis of lymphoid tissues, including PPs and pLNs (Kiyono and Fukuyama, 2004). However, NALT does not follow the general biological rule of the dependence of embryonic genesis on inflammatory cytokines (Fukuyama et al., 2002; Harmsen et al., 2002). NALT organogenesis, which occurs postnatally, is independent of LTβR-mediated signals and RORγt but does require Id2 (Fukuyama et al., 2002; Harmsen et al., 2002).

In this study, we provide evidence that TALT develops independently of organogenesis regulators, a finding that distinguishes TALT genesis from that of other lymphoid organs. In addition, we found that TALT plays a central role in the induction of antigen-specific immune responses against ocularly encountered antigens.

RESULTS

Identification of TALT in mice

TALT develops in the human tear duct (Knop and Knop, 2000, 2001; Paulsen et al., 2000, 2003), but to our knowledge no information is currently available on TALT in mice. To identify organized lymphoid tissue in the mouse tear duct and to elucidate its immunological and developmental features, we first examined the anatomy of this duct in mice. To visualize the position of the tear duct, we administered hematoxylin to mice in eye drops. We clearly observed the location of the tear duct where it connects the ocular surface to the nasal cavity (Fig. 1 A). In coronal and horizontal views, we were able to identify TALT in both the left and right side of the lacrimal sac in C57BL/6 WT mice (Fig. 1, B and C).

Postnatal development of TALT

The genesis of each type of lymphoid tissue occurs within a given time window: for example, PPs develop during late embryogenesis and NALT develops postnatally (Fukuyama et al., 2002; Mebius, 2003; Kiyono and Fukuyama, 2004). The initiation of intestinal isolated lymphoid follicles (ILFs) also occurs after birth, and the genetic background (e.g., whether the mouse is of the C57BL/6 or BALB/c strain) influences the postnatal time of initiation of tissue genesis (Hamada et al., 2002). To determine when TALT genesis is initiated and to evaluate the influence of genetic background on tissue genesis, we took tissue samples from both C57BL/6 and BALB/c mice at various pre- and postnatal stages for histological analysis. No sign of mononuclear cell accumulation was observed at embryonic day (E) 18 or postnatal day (D) 5 in C57BL/6 or BALB/c mice (Fig. 1 D and Fig. S1). In contrast, we detected accumulation of mononuclear cells at D10 in both C57BL/6 and BALB/c mice, indicating that the TALT development was initiated between D5 and D10, and that the different genetics of the two strains did not influence TALT organogenesis (Fig. 1 D and Fig. S1). To support the data, the initial appearance of mononuclear cells was noted at D7 in both C57BL/6 and BALB/c mice (Fig. 1 D and Fig. S1). Furthermore, pLN addressin (PNAd)–positive high endothelial venules (HEVs) developed at D10 but not at D5 and D7 (Fig. 1 E). These findings suggest that TALT develops postnatally, as does NALT. Unlike in the genesis

of other lymphoid tissues (Mebius, 2003), expression of vascular cell adhesion molecule 1 (VCAM-1) was not observed at the TALT anlage (unpublished data).

To determine which cell population initially migrates to the TALT anlage, we analyzed the tissue genesis site at D5, D7, and D10 by confocal microscopy. The D5 anlagen did not

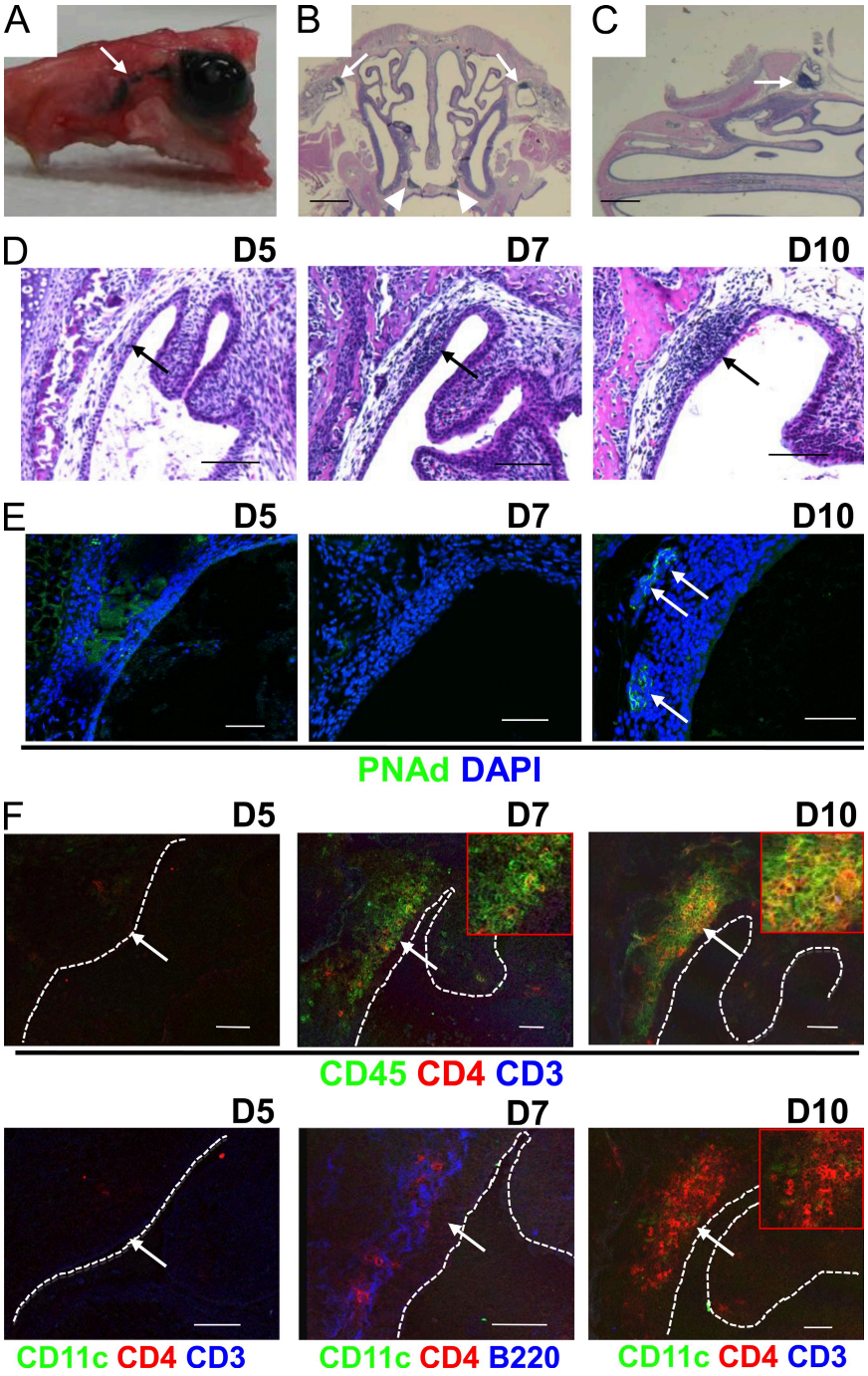

Figure 1. Postnatal development of TALT. (A–C) 10 µl of hematoxylin solution was added to the ocular surface of 8-wk-old C57BL/6 mice to visualize the tear duct (A, arrow). Coronal (B) and horizontal (C) paraffinized sections of the head were stained with HE. Arrows and arrowheads indicate TALT and NALT, respectively (n = 3 mice/group). Bars, 1 mm. (D) Paraffinized tissues of heads from D5, D7, and D10 C57BL/6 mice were examined by HE staining. Arrows indicate the site of TALT genesis (n = 5 mice/group). Bars, 100 µm. (E and F) Head tissue of C57BL/6 mice was examined by confocal microscopy with the indicated antibodies at D5, D7, and D10. Arrows indicate PNAd$^+$ HEVs (E) and the site of TALT genesis (F). Some magnified pictures are shown in F (insets). Dashed lines indicate the edge between the TALT epithelium and tear duct lumen. These data are representative of at least three independent experiments (n = 5 mice/group). Bars, 50 µm.

contain any CD45$^+$ cells, whereas the D7 TALT anlage possessed CD45$^+$ cells (Fig. 1 F). CD3$^-$CD4$^+$CD45$^+$ cells have been shown to be LTi cells (Mebius, 2003). Among the CD45$^+$ cells in the D7 TALT anlage, we identified CD3$^-$CD4$^+$CD45$^+$ cells and B220$^+$ B cells (Fig. 1 F, D7). CD11c$^+$ DCs were not found at D5 and D7. At D10, CD11c$^+$ DCs and increased numbers of CD3$^-$CD4$^+$CD45$^+$ cells were found in the TALT (Fig. 1 F). Because B220$^+$ B cells were among the first cells to migrate at the TALT anlage (Fig. 1 F, D7), we examined B cell–deficient *Igh6*$^{-/-}$ mice for the development of TALT. The TALT genesis occurred normally, even in the B cell–deficient condition (Fig. S2 A). Further, TALT also developed in T cell–deficient *Tcrβ*$^{-/-}$, *Tcrδ*$^{-/-}$ mice (Fig. S2 B). These findings show that B and T lymphocytes and DCs are dispensable for the initiation of TALT development.

Organogenesis of TALT does not require microbial stimulation

TALT has been identified in only 30–40% of humans examined (Paulsen et al., 2000, 2003; Knop and Knop, 2001), raising the possibility that environmental conditions, including microbial infections and allergic responses, are involved in the initiation of TALT development. In addition, our finding that TALT develops postnatally also points to the possible involvement of microbial stimulation in TALT genesis. However, we detected TALT in mice deficient in Toll-like receptor (TLR) signals, including *Tlr2*$^{-/-}$, *Tlr4*$^{-/-}$, and *MyD88*$^{-/-}$ mice (Fig. S2, C–E). Further, we found that germ-free mice developed TALT (Fig. 2 A). Thus, TALT organogenesis is most likely independent of microbial stimulation.

TALT development is independent of organogenesis regulators

We next determined the molecular requirements for TALT development. PPs and pLNs are not present in alymphoplasia (*aly/aly*) mice, which carry a null mutation of NF-κB–inducing kinase (NIK), resulting in a failure to transmit LTβR-mediated signals (Shinkura et al., 1999). However, our histological analysis showed that the TALT structure was preserved in *aly/aly* and *Ltα*$^{-/-}$ mice, although it was smaller than in WT TALT (Fig. 2, A and B; and Fig. S3). In addition, TALT was even observed in *Il-7rα*$^{-/-}$ mice, although the size was again small (Fig. 2 B and Fig. S3). Thus, the initiation of TALT development mediated by inducer cells was independent of the IL-7R and LTα1β2–LTβR–NIK pathway signaling cascades, whereas the maturation process of accumulating lymphocytes required the cytokine signaling cascade, as is the case with other lymphoid organs (Mebius, 2003; Kiyono and Fukuyama, 2004).

Lymphoid chemokines, including CXCL13, CCL19, and CCL21, play important roles in the migration of LTi cells to the sites of tissue genesis (Honda et al., 2001; Luther et al., 2003; Fukuyama et al., 2006). We therefore examined the involvement of these lymphoid chemokines in TALT genesis. The TALT structure was preserved in *Cxcl13*$^{-/-}$ mice, although they lacked some pLNs and had reduced numbers of PPs (Fig. 2 B; Ansel et al., 2000). TALT also developed well in *plt/plt* mice (Fig. 2 B), which carry null mutations of both the *Ccl19* and *Ccl21* genes (Nakano et al., 1998). Furthermore, the initiation of TALT formation was maintained in triple mutant (*Cxcl13*$^{-/-}$ *plt/plt*) mice (Fig. 2 B), confirming that these lymphoid chemokines are not required for the initiation of TALT organogenesis, although the TALT was smaller in the lymphoid chemokine–null condition than in WT (Fig. S3). These results supported the observation that an NIK-mediated pathway is required to recruit large numbers of lymphocytes to TALT.

We then addressed the involvement of Id2 and RORγt, key transcriptional regulators in the induction of lymphoid organogenesis by CD3$^-$CD4$^+$CD45$^+$ LTi cells (Yokota et al., 1999; Sun et al., 2000; Eberl et al., 2004). Surprisingly, TALT formation was preserved in *Id2*$^{-/-}$ and *Rorγt*$^{-/-}$ mice (Fig. 2 B). Consistent with this finding, FACS and confocal microscopy analyses detected CD3$^-$CD4$^+$ LTi cells in the TALT anlage of *Id2*$^{-/-}$ and *Rorγt*$^{-/-}$ mice as well as in WT mice (Fig. 3, A and B). Furthermore, when we isolated these CD3$^-$CD4$^+$CD45$^+$ cells from WT mice and examined the gene expression of the tissue genesis–associated transcription factors by RT-PCR, we found that CD3$^-$CD4$^+$CD45$^+$ cells isolated from the TALT anlagen did not express either *Id2* or *Rorγt*, whereas CD3$^-$CD4$^+$CD45$^+$ cells isolated from the embryonic intestine, i.e., PP inducer cells, expressed both *Id2* and *Rorγt* (Fig. 3 C). Thus, TALT organogenesis proceeds independently of Id2, RORγt, and LT. Therefore, TALT genesis is quite different from the genesis of other secondary lymphoid tissues, including PPs, pLNs, and NALT (Mebius, 2003; Kiyono and Fukuyama, 2004).

Microarchitecture of TALT

The structure of the MALT epithelium is characterized by the presence of follicle-associated epithelium (FAE; Kiyono and Fukuyama, 2004). Indeed, we were able to divide the epithelial layer of the lacrimal sac into two populations on the basis of its morphological structure (Fig. 4 A): TALT-FAE was characterized by a thin layer of squamous epithelium (Fig. 4 B), whereas the lacrimal sac epithelium had a multilayered and squamous morphology (Fig. 4 C). Interestingly, TALT-FAE lacked mucus-producing goblet cells and cilia (Fig. 4 B), a fact that distinguished this tissue from NALT-FAE, which has some goblet cells (Fig. 4 D). Instead, mucus-producing gland tissue was frequently observed on the conjunctiva (unpublished data). Confocal microscopic analysis of TALT revealed large numbers of B220$^+$ B cells (Fig. 4 E) and CD11c$^+$ DCs in the subepithelial dome region of the FAE (Fig. 4 F), as well as CD3$^+$CD4$^+$ T helper cells distributed around the B cell follicles (Fig. 4, G and H). These data indicate that TALT is composed of a highly compartmentalized and organized lymphoid structure. In accordance with the finding that neonatal TALT developed PNAd$^+$ HEVs (Fig. 1 E), adult TALT HEVs expressed PNAd but not mucosal addressin cell adhesion molecule 1 (MAdCAM-1; Fig. 4 I and Fig. S4 A); this is similar to the case with NALT HEVs

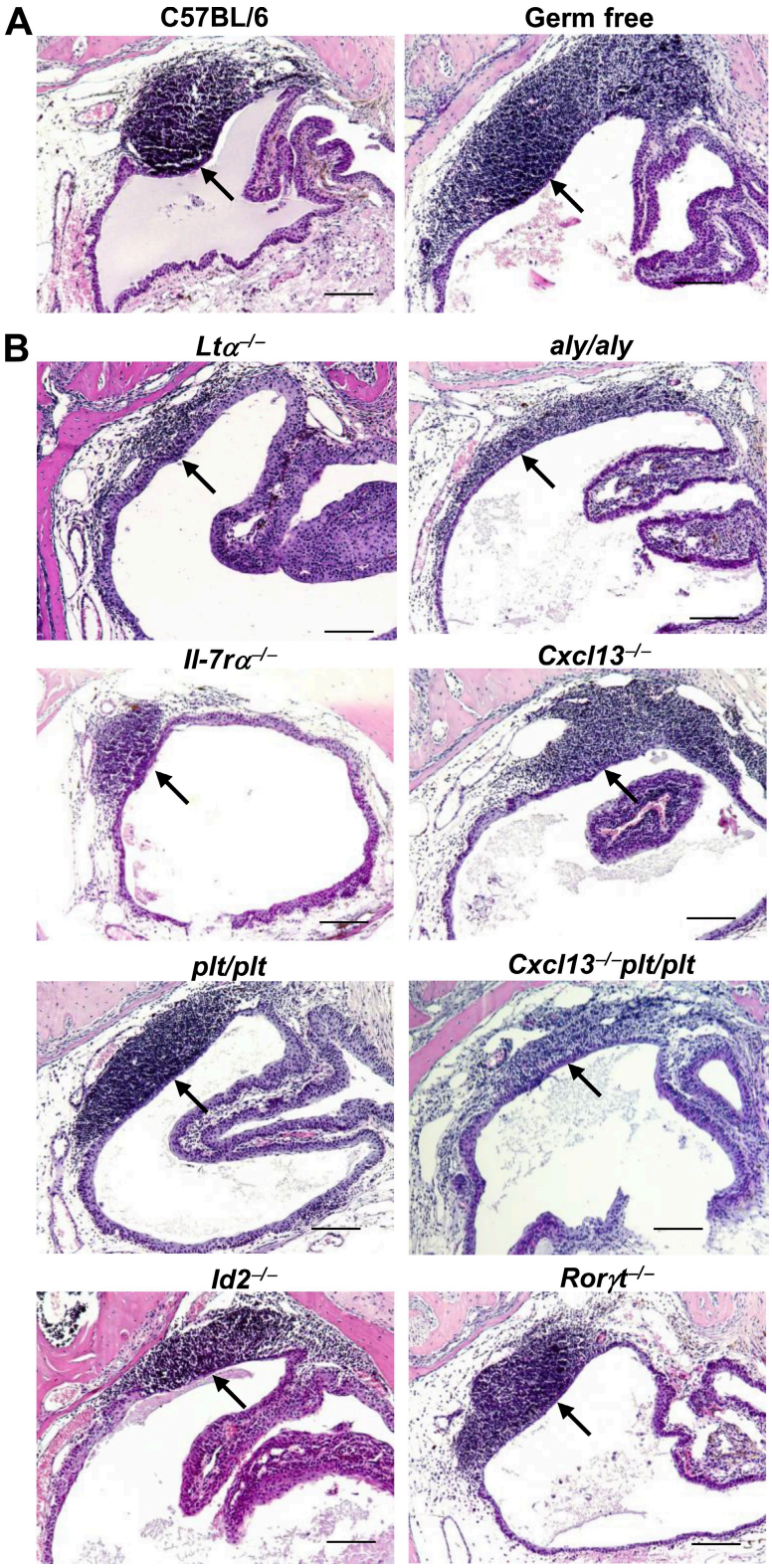

Figure 2. TALT genesis is independent of microbial stimulation and organogenesis-associated molecules. Paraffin-embedded tissue sections were analyzed by HE staining for TALT development. (A) The presence of TALT in germ-free mice, as well as C57BL/6 WT mice, shows that TALT develops independently of microbial stimulation ($n = 3$ mice/group). (B) Development of TALT in 8-wk-old *Ltα*$^{-/-}$, *aly/aly*, *Il-7rα*$^{-/-}$, *Cxcl13*$^{-/-}$, *plt/plt*, *Cxcl13*$^{-/-}$*plt/plt*, *Id2*$^{-/-}$, and *Rorγt*$^{-/-}$ mice shows that the initiation of TALT development occurs independently of organogenesis-associated molecules. Arrows indicate the presence of TALT. These data are representative of at least three independent experiments per group ($n = 5$ mice/group). Bars, 100 µm.

(Fig. 4 J and Fig. S4 B). These observations suggest that cellular trafficking to TALT and NALT is regulated via an L-selectin–PNAd interaction and is distinguishable from gut-trafficking mechanisms, which are dependent on α4β7 integrin/MAdCAM-1 (Kiyono and Fukuyama, 2004). These results indicate that TALT possesses many of the characteristic traits of organized MALT but is distinguished by the lack of goblet cells in its FAE region.

TALT is a site of immunological induction

To investigate the physiological function of TALT, we examined whether TALT takes up ocularly administered antigens. M cells, characterized by the M cell–specific mAb NKM16-2-4$^+$ (Nochi et al., 2007), *Ulex europaeus* agglutinin (UEA) 1$^+$, and wheat germ agglutinin$^-$, were found in the FAE of TALT (Fig. 5 A). Electron microscopic analysis showed that TALT-FAE contained cells bearing the hallmarks of M cells: microvilli and a unique pocket formation with lymphocytes (Fig. 5, B and C). When mice were ocularly dosed with GFP-expressing *Salmonella*, we observed the uptake of *Salmonella* by UEA-1$^+$ M cells (Fig. 5 D) as well as by CD11c$^+$ DCs (Fig. 5 E). Moreover, when mice were ocularly challenged with *Pseudomonas aeruginosa* PAO1, large amounts of *P. aeruginosa* PAO1 were located within the TALT (Fig. 5 F). *P. aeruginosa* PAO1 was not detected in naive mice (Fig. 5 G). Mice ocularly challenged with *P. aeruginosa* PAO1 formed germinal centers (GCs; Fig. 5 H); this is an important immunological event for the initiation of hypersomatic mutations and Ig class switching, which enable the production of memory B cells with high-affinity B cell receptors (Kelsoe, 1996; Shapiro-Shelef and Calame, 2005). In contrast, GC formation was not present in the TALT of naive mice (Fig. 5 I; and Fig. 6, A and B). These data suggest that TALT is a preferential site for the uptake of ocularly encountered antigens/pathogens and for the subsequent induction of antigen-specific B cell responses.

Supporting this notion, immunization of the eyes with eye drops containing cholera toxin (CT), a well-known mucosal immunogen, resulted in the formation of GCs with a follicular DC (FDC) network in the TALT (Fig. 6, C and D). Interestingly, ocular immunization also induced GC formation in NALT (Fig. 6, E and F), suggesting that the anatomical

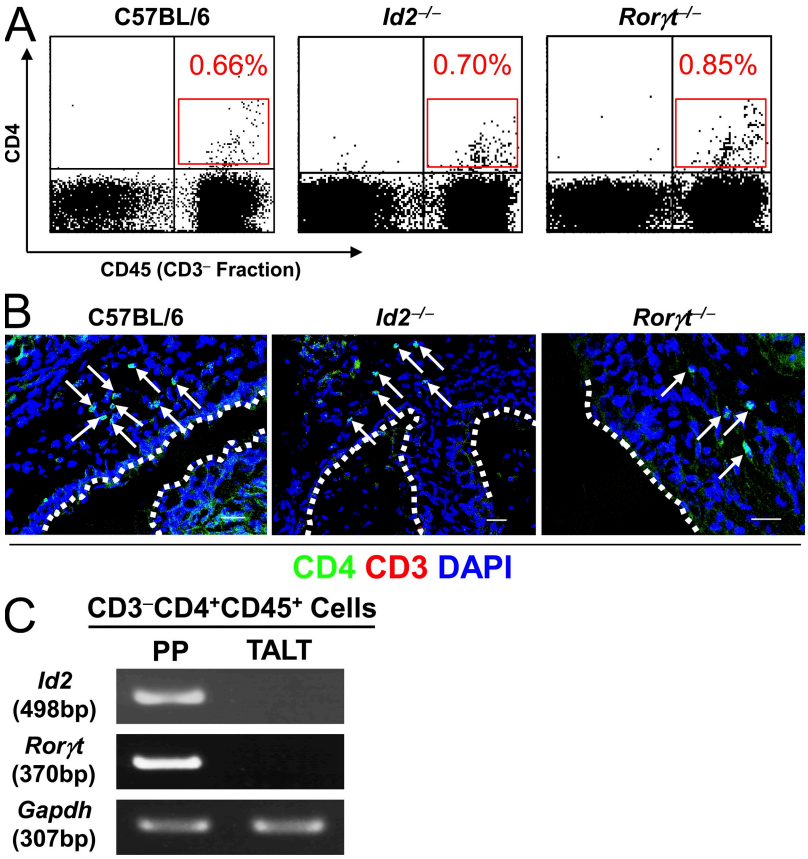

Figure 3. Presence of CD3$^-$CD4$^+$CD45$^+$ cells in the TALT anlagen. (A) Because substantial numbers of CD3$^-$CD4$^+$CD45$^+$ cells were noted in the TALT anlagen of D10 mice, we analyzed mononuclear cells from D10 tear ducts by FACS. Percentages of CD3$^-$CD4$^+$CD45$^+$ cells are shown in red (n = 6 mice/group). (B) Confocal microscopic analysis of the site of TALT genesis at D10. Frozen tissue samples were stained with the antibodies indicated. Arrows point to CD3$^-$CD4$^+$ cells (n = 6 mice/group). Dotted lines indicate the edge between the TALT epithelium and tear duct lumen. Bars, 50 µm. (C) CD3$^-$CD4$^+$CD45$^+$ cells from PP and TALT were isolated from an E17 intestine and D10 tear duct, respectively. Gene expression of *Id2* and *Rorγt* were analyzed by RT-PCR. The expression of *Gapdh* is shown as an internal control. These data are representative of at least three independent experiments (n = 18–20 mice/group).

connection through the tear duct lays the groundwork for a cooperative immunological network between TALT and NALT that responds to ocularly encountered antigens. Activation-induced cytidine deaminase (AID), an essential Ig class switch–related molecule, is expressed in organized lymphoid tissues, including NALT, PPs, and intestinal ILFs (Shikina et al., 2004). Parallel to our findings of GC formation after ocular immunization, confocal microscopy revealed the presence

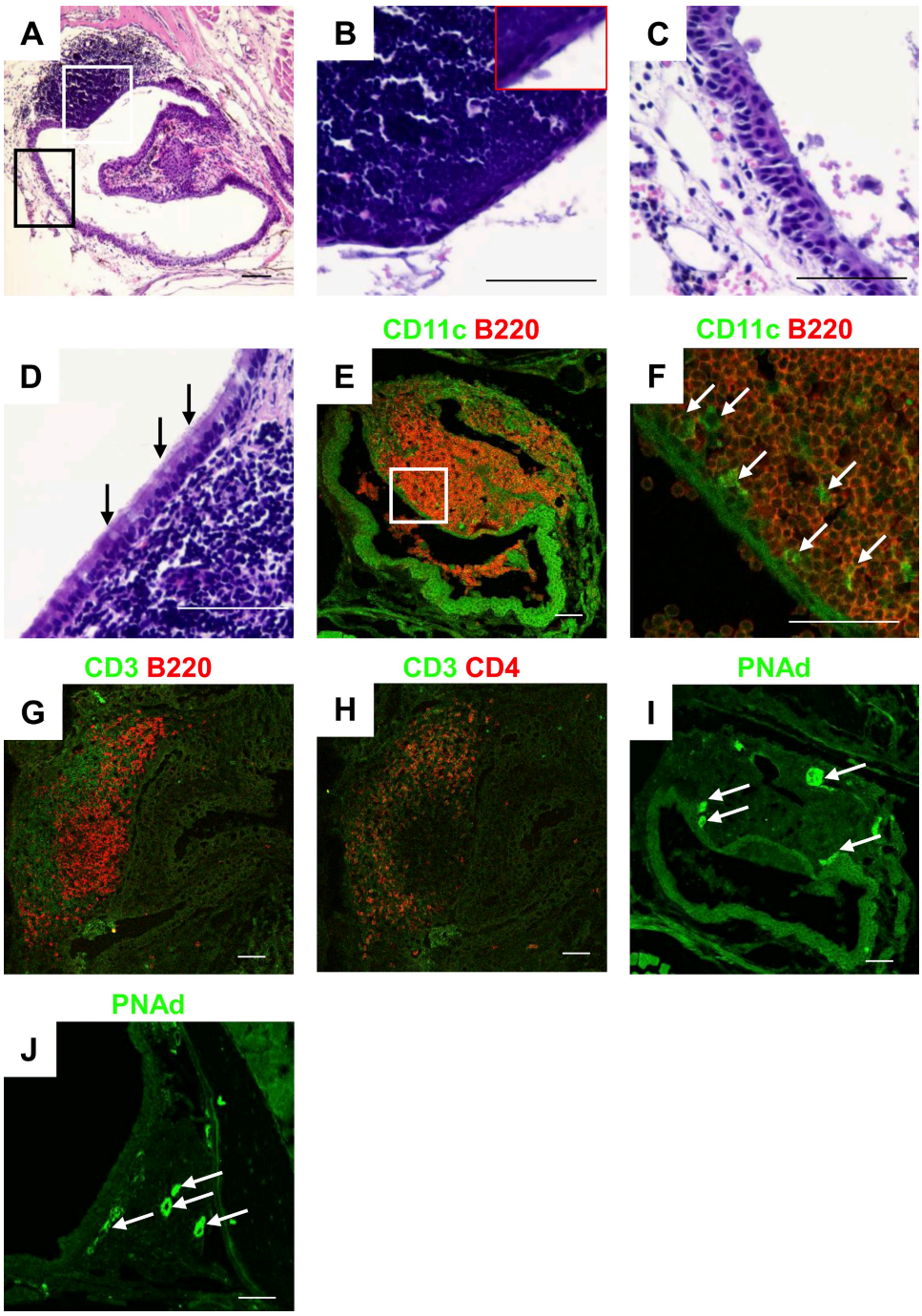

Figure 4. Microarchitecture of TALT. (A–C) The epithelial region of TALT in WT mice was analyzed by HE staining. B and C are magnifications, respectively, of the white and black boxes in A, and show TALT-FAE (B) and the lacrimal sac epithelium (C). The inset in B shows single-layered squamous epithelium in the TALT FAE (n = 3 mice/group). (D) The presence of goblet cells in NALT-FAE is indicated by arrows (n = 3 mice). (E–J) Confocal microscopic analysis of TALT (E–I) and NALT (J) in C57BL/6 WT mice. Tissue samples were stained with the antibodies indicated. F is a magnified view of the box in E; arrows point to the presence of CD11c$^+$ DCs. Arrows in I and J indicate PNAd$^+$ HEVs. These data are representative of at least three independent experiments (n = 3 mice/group). Bars, 50 µm.

of AID-expressing cells in both TALT and NALT (Fig. 6, G, and H). Furthermore, RT-PCR analysis confirmed *Aid* expression in TALT and NALT but not in the nasal passage (NP; Fig. 6 I). Therefore, after ocular immunization with CT, increased numbers of IgA^+B220^- plasma cells were detected in the diffuse region of the tear duct (Fig. 6, J and K). An ELISPOT assay confirmed that some of these IgA^+B220^- plasma cells produced CT-specific IgA; cells producing IgA specific for the B subunit of CT (CT-B), but not IgG-forming cells, were found in single-cell preparations from the tear ducts of mice ocularly immunized with CT (Fig. 6 L and not depicted). In addition, the production of CT-B–specific IgG-forming cells was induced in the spleen by ocular immunization with CT (Fig. 6 M). Naive mice did not show any CT-B–specific Ig-producing cells (Fig. 6 N).

In addition, we found a high frequency of CT-B–specific $CD4^+$ T cells in TALT using an MHC tetramer, consistent with the induction of antigen-specific antibody-producing

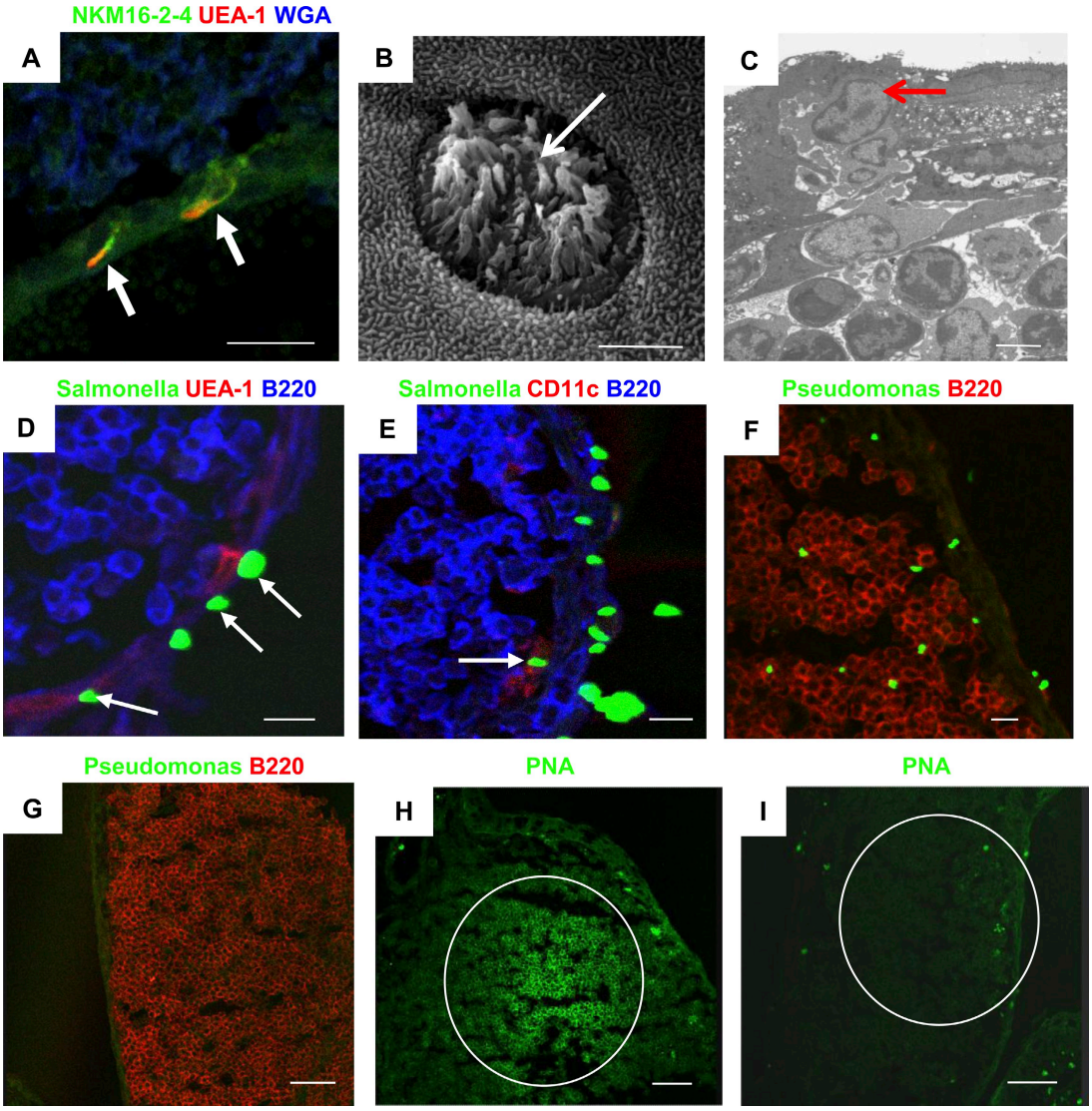

Figure 5. TALT is the site of ocular antigen uptake. (A) A confocal micrograph of TALT shows the presence of $NKM16\text{-}2\text{-}4^+$ $UEA\text{-}1^+$ M cells (arrows; $n = 3$ mice). Bar, 20 µm. (B and C) TALT-FAE was analyzed by scanning electron microscopy (B) and transmission electron microscopy (C). White and red arrows indicate M cells with the unique characteristics of microvilli and pocket lymphocytes, respectively ($n = 5$ mice/group). Bars, 3 µm. (D and E) Mice were given GFP-expressing *Salmonella* by eye drops. After 30 min, TALT was isolated and examined with confocal microscopy. Arrows in D and E point, respectively, to *Salmonella* captured by $UEA\text{-}1^+$ M cells and $CD11c^+$ DCs in TALT ($n = 3$ mice/group). Bars, 10 µm. (F) Mice were given *P. aeruginosa* PAO-1 by eye drops. After 30 min, TALT was isolated and examined with confocal microscopy. A large number of *P. aeruginosa* PAO-1 were found inside the TALT ($n = 3$ mice). Bar, 10 µm. (G) As a negative control for F, TALT from mice given PBS by eye drops were analyzed ($n = 3$ mice). Bar, 50 µm. (H) Mice were given *P. aeruginosa* PAO-1 by eye drops twice at an interval of 1 wk. 1 wk after the second administration, TALT was isolated and examined with confocal microscopy. GC formation was induced by ocular administration of *P. aeruginosa* PAO-1 ($n = 3$ mice). Bar, 50 µm. (I) TALT from a control naive mouse is shown. GCs did not form in naive TALT. These data are representative of at least two independent experiments per group ($n = 3$ mice). Bar, 50 µm.

cells after CT immunization (Fig. 7 A). It is important to note that the CT-B tetramer–reactive $CD4^+$ T cells included $CXCR5^+$ T follicular helper cells (Fig. 7 B). CT-B–specific $CD4^+$ T cells were detected in NALT and draining LNs, such as the cervical and submandibular LNs, but at a lower frequency than in TALT (Fig. 7, A and B). Thus, it is plausible

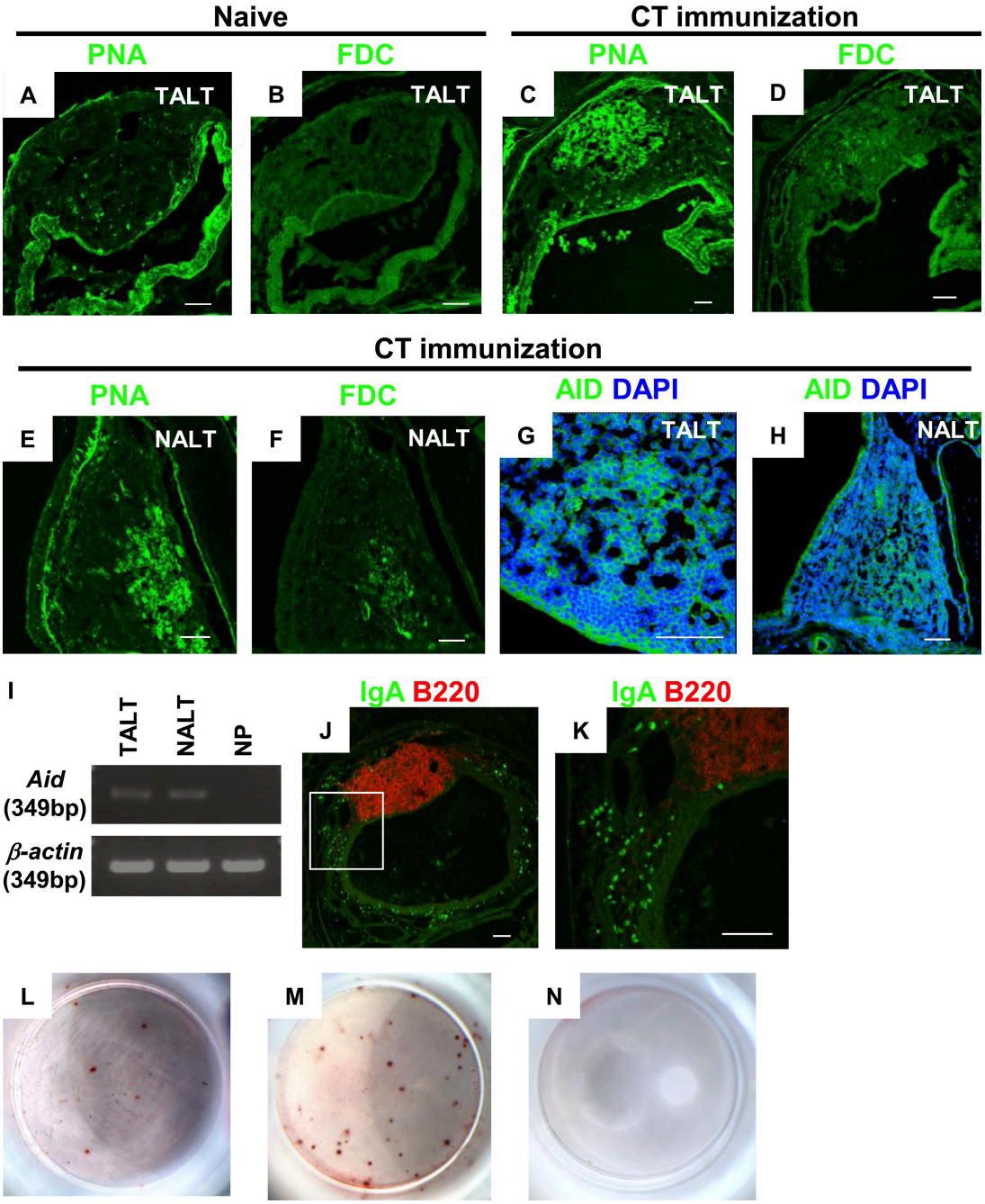

Figure 6. Induction of antigen-specific IgA responses through TALT. (A and B) Naive mice do not form GCs ($n = 3$ mice). (C and D) Mice were given CT by eye drops three times at 1-wk intervals. 1 wk after the last administration, TALT was isolated and examined with confocal microscopy. The CT challenge induced GC formation in TALT (C and D) and NALT (E and F; $n = 3$ mice/group). Tissues were stained with PNA (A, C, and E) or for FDCs (B, D, and F). (G and H) AID expression in TALT (G) and NALT (H) was detected in mice ocularly immunized with CT ($n = 3$ mice/group). (I) RT-PCR analysis of *Aid* expression in TALT, NALT, and NPs of mice given ocular CT ($n = 3$ mice/group). (J and K) Distribution of IgA^+B220^- plasma cells in tear ducts was examined with confocal microscopy. K is a magnified view of the box in J. CT challenge by eye drops induced the appearance of a large number of plasma cells in the tear duct compartment ($n = 3$ mice/group). (L–N) ELISPOT analysis for the detection of CT-B–specific IgA-producing cells in tear ducts (L) and CT-B–specific IgG-producing cells in spleens (M). Data obtained from control naive mice are shown in N. These data are representative of at least two independent experiments ($n = 4$ mice/group). Bars, 50 µm.

that TALT is the main gateway and inductive site for the initiation of antigen-specific T and B cell responses against ocularly encountered antigens. Collectively, these observations indicate that TALT is an important member of the MALT family. It has a lymphoid structure that is organized as an inductive site for antigen uptake and the initiation of antigen-specific mucosal immune responses with GC formation and Ig class switching, as well as the generation of antigen-specific $CD4^+$ T cells.

DISCUSSION

Our purpose was to investigate the developmental features of TALT and to reveal the immunological importance of this tissue in immune surveillance for mucosal immunity. We found that the molecular requirements of TALT organogenesis were quite different from those of other secondary lymphoid organs. For example, the initiation of TALT organogenesis is independent of the IL-7R– and LTβR–NIK–mediated tissue genesis pathways, and thus, its structure was preserved in mice lacking other secondary lymphoid organs, such as *Il-7rα*$^{-/-}$, *Ltα*$^{-/-}$, and *aly/aly* mice (Table I). Furthermore, the TNF-related activation-induced cytokine (TRANCE)–mediated pathway, which is involved in pLN development (Kong et al., 1999), was dispensable for TALT genesis. Thus, the TALT structure was found in *Trance*$^{-/-}$ mice and in mice null for its signal transducer, TNF receptor–associated factor (TRAF) 6 (Fig. S5). However, these mice lacking secondary lymphoid organs (e.g., *Il-7rα*$^{-/-}$, *Ltα*$^{-/-}$, and *aly/aly* mice) had smaller TALT volumes than were found in WT mice. LTβR–NIK–mediated signals induce the production of lymphoid chemokines such as CXCL13, CCL19, and CCL21, and adhesion molecules, including VCAM-1 and PNAd (Dejardin et al., 2002; Browning et al., 2005). The immature formation of TALT in mice deficient in LTβR-associated molecules can therefore be explained by the lack of lymphoid chemokines and adhesion molecules involved in leukocyte migration. In support of this, the extent of the TALT in *Cxcl13*$^{-/-}$*plt/plt* mice was smaller than that in *Cxcl13*$^{-/-}$ and *plt/plt* single- or double-mutant mice, as well as in WT mice. However, accumulation of some B lymphocytes was seen in these mutant mice (Fig. S3). Thus, we cannot eliminate the possibility that the migration stage of B lymphocytes may also operate independently of the LTβR–NIK pathway for TALT genesis.

One of the important findings of our study is that TALT genesis occurs in both *Id2*$^{-/-}$ and *Rorγt*$^{-/-}$ mice. TALT genesis takes place normally in *Rorγt*$^{-/-}$ mice despite the fact that $CD3^-CD4^+CD45^+$ LTi cells, and as a consequence PPs and pLNs, are totally absent in these mice (Sun et al., 2000; Eberl et al., 2004). In addition, Id2 is the key transcriptional regulator for the induction and differentiation of $CD3^-CD4^+CD45^+$ LTi cells (Yokota et al., 1999). *Id2*$^{-/-}$ mice do not develop any form of secondary lymphoid tissues, including pLNs, PPs, or NALT (Yokota et al., 1999; Fukuyama et al., 2002). However, TALT development is Id2 and RORγt independent (Table I). We still found that $CD3^-CD4^+CD45^+$ cells, which we hypothesize to be TALT inducer cells, existed at TALT anlagen in both *Id2*$^{-/-}$ and *Rorγt*$^{-/-}$ mice, and we revealed that $CD3^-CD4^+CD45^+$ cells isolated from TALT anlagen did not express either *Id2* or *Rorγt*. A recent study showed that omental milky spots developed in the absence of LTi cells (Rangel-Moreno et al., 2009). Omental milky spots were found in *Id2*$^{-/-}$ and *Rorγt*$^{-/-}$ mice. However, this tissue development required the lymphoid chemokine CXCL13. Because the initiation of TALT development is independent of CXCL13, omental milky spots and TALT use different tissue

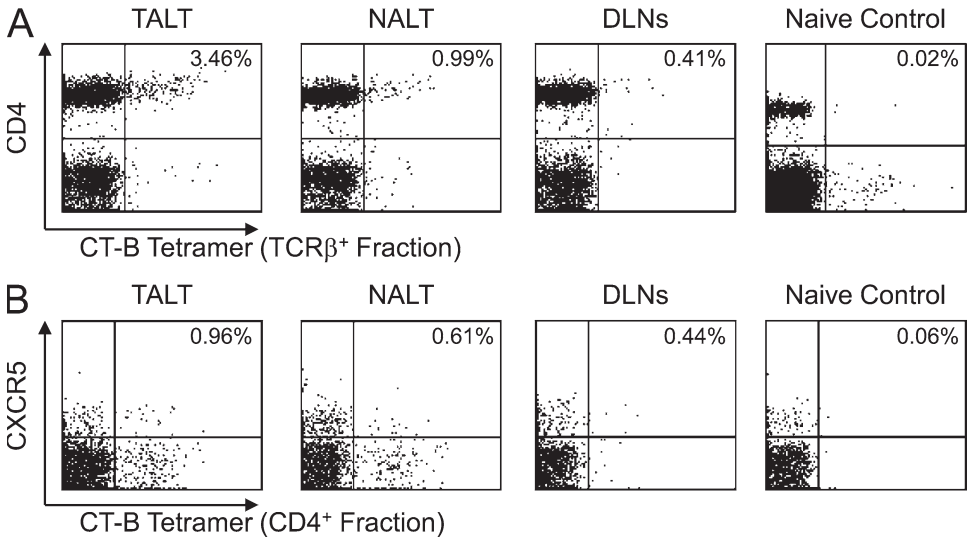

Figure 7. Induction of antigen-specific $CD4^+$ T cell responses in TALT after ocular immunization. (A and B) FACS analysis of CT-B tetramer–positive cells in lymphocytes isolated from TALT, NALT, and draining LNs (DLNs; cervical and submandibular LNs) of CT-immunized or naive mice. Data from $TCR\beta^+$ (A) and $CD4^+$ (B) populations are shown. TALT preferentially responded to ocular administration of CT and generated CT-B–specific $CD4^+$ T cells, including $CXCR5^+$ T follicular helper cells. These data are representative of at least two independent experiments (n = 4 mice/group).

Table I. Distinct molecular features for organogenesis of different MALTs

Mice	TALT	NALT	PP	CLN	MLN	ILF	Cryptopatch	References
Id2$^{-/-}$	+++	−	−	−	−	ND	ND	*1
Rorγt$^{-/-}$	+++	+++	−	−	−	−	+/−	*2
Lt$\alpha^{-/-}$	+	+	−	−	+/−	−	+/−	*3
aly/aly	+	+	−	−	−	−	++	*4
Il-7r$\alpha^{-/-}$	++	++	−	+/−	++	++	−	*5
Cxcl13$^{-/-}$	++	+	+/−	+/−	++	ND	ND	*6
plt/plt	+++	++	++	++	++	ND	ND	*7
Cxcl13$^{-/-}$ *plt/plt*	+	+	+/−	−	++	ND	ND	*8

CLN, cervical LN; MLN, mesenteric LN. +++, developed well; ++, developed with decreased number of lymphocytes; +, developed with few number of lymphocytes; −, absent; +/−, present or absent, depends on individual. *1, Yokota et al., 1999; Fukuyama et al., 2002; Boos et al., 2007; *2, Sun et al., 2000; Harmsen et al., 2002; Eberl and Littman, 2004; Eberl et al., 2004; Naito et al., 2008; Tsuji et al., 2008; *3, De Togni et al., 1994; Banks et al., 1995; Suzuki et al., 2000; Fukuyama et al., 2002; Hamada et al., 2002; Harmsen et al., 2002; Taylor et al., 2004; *4, Kanamori et al., 1996; Shinkura et al., 1999; Fukuyama et al., 2002; Hamada et al., 2002; *5, Peschon et al., 1994; Kanamori et al., 1996; Adachi et al., 1998b; Fukuyama et al., 2002; Hamada et al., 2002; Luther et al., 2003; *6, Ansel et al., 2000; Rangel-Moreno et al., 2005; Fukuyama et al., 2006; *7, Nakano et al., 1997; Rangel-Moreno et al., 2005; Fukuyama et al., 2006; and *8, Luther et al., 2003; Rangel-Moreno et al., 2005; Fukuyama et al., 2006.

genesis mechanisms. The organogenesis of secondary lymphoid tissues has been shown to require several processes, including the trafficking/accumulation of LTi cells, the differentiation/activation of specialized stromal cells, and the trafficking/accumulation of conventional lymphocytes (Mebius, 2003). In this light, the genesis of these tissues can be separated into at least two phases, initiation and maturation; in other words, the migration of LTi cells and lymphocytes, respectively, to the tissue development site. Our results indicate that the initiation of TALT genesis operates independently of the requirement for the classical tissue genesis–associated signaling cascade of IL-7R/LTβR–NIK because leukocytes, including B lymphocyte, already migrated to TALT without this pathway. Further, the unique $CD3^-CD4^+CD45^+$ cells develop without a requirement for the LTi cell–associated transcriptional regulators Id2 and RORγt, and are identified as the first hematopoietic cell population that migrates to the TALT anlagen. To directly address the critical role of Id2- and RORγt-independent $CD3^-CD4^+CD45^+$ cells (or TALT inducer cells) in the initiation of TALT genesis, our efforts are now directed toward finding and/or developing TALT-deficient mice for the necessary adoptive transfer experiment.

TALT organogenesis occurs after birth, as does NALT genesis (Fukuyama et al., 2002). In contrast, PPs and pLNs are initially generated during the embryonic period (Mebius, 2003). These findings suggest that secondary lymphoid tissue genesis can be chronologically separated into two categories: a prenatal group (PPs and pLNs) and a postnatal group (TALT and NALT). However, initiation of genesis of all of these tissues, including TALT, occurs independently of microbial stimuli.

Ocular surface antigens are taken up by NALT, and NALT might function as an inductive site for tear IgA production (Ridley Lathers et al., 1998). However, our findings suggest that TALT is a key inductive tissue for immune responses, because TALT is a more important site for the generation of antigen-specific T cells than NALT and, thus, contributes to mucosal immune responses against ocularly encountered antigens. In support of this suggestion, our study showed the presence of a mucosal gateway population of M cells in TALT that is capable of taking up ocularly administered bacterial antigens (e.g., *Salmonella*). Ocular infection with *P. aeruginosa* causes corneal ulcers and sometimes loss of vision (Liesegang, 1998), and we found *P. aeruginosa* given by ocular challenge within TALT, leading to the subsequent formation of GCs. These findings indicate that TALT plays an important role in ocular immune surveillance and protection, providing the first line of defense of the host's eyesight; we can therefore expect it to be equivalent in its capacity for immunosurveillance to the other well-known mucosal inductive tissues in the aerodigestive tract, NALT and PPs.

The lacrimal glands are effector sites for IgA production because their tissue contains large numbers of IgA-producing cells (Sullivan and Allansmith, 1984; Peppard and Montgomery, 1987; Saitoh-Inagawa, 2000). We also found that a large number of IgA^+B220^- plasma cells were distributed around the diffuse tissues of the NPs and in the tear duct in response to CT immunization via eye drops. Thus, TALT and various tissues of the tear duct are responsible for ocular immunity as inductive and effector sites, respectively.

In summary, our results demonstrated the presence of mouse TALT, providing the first definitive evidence for the existence of Id2-, RORγt-, and LTβR-independent lymphoid tissue genesis. In addition, TALT was shown to play an important role in the induction of antigen-specific immune responses and to function in immune surveillance in ocular immunity.

MATERIALS AND METHODS

Mice. C57BL/6 and BALB/c mice were purchased from Japan SLC; germ-free and *aly/aly* mice were purchased from CLEA Japan; and *Lt*$\alpha^{-/-}$, *Igh6*$^{-/-}$, *Tcr*$\beta^{-/-}$, and *Tcr*$\delta^{-/-}$ mice were purchased from the Jackson Laboratory. *Il-7r*$\alpha^{-/-}$ mice were provided by Immunex Corp., and were also purchased from the Jackson Laboratory. *Id2*$^{-/-}$, *Rorγt*$^{-/-}$, *Cxcl13*$^{-/-}$, *Tlr2*$^{-/-}$, *Tlr4*$^{-/-}$, *MyD88*$^{-/-}$, *Cxcl13*$^{-/-}$*plt/plt*, *Trance*$^{-/-}$, and *Traf6*$^{-/-}$ mice were generated as previously described (Adachi et al., 1998a; Hoshino et al., 1999; Kong et al., 1999; Naito et al., 1999; Takeuchi et al., 1999;

Yokota et al., 1999; Kurebayashi et al., 2000; Ebisuno et al., 2003; Fukuyama et al., 2006). Animal experiments were conducted in accordance with the guidelines of and with permission provided by the Animal Care and Use Committee of the University of Tokyo.

Histological analysis. Histological analysis was performed as previously described (Fukuyama et al., 2002). The antibodies and lectins used for confocal microscopy analysis were as follows: FITC– or PE–anti-CD11c (HL3; BD), FITC–anti-CD3ε (145-2C11; BD), FITC–anti-IgA (C10-3; BD), PE–anti-B220 (RA3-6B2; BD), PE–anti-CD45 (30-F11; BD), PE– or APC–anti-CD4 (RM4-5; BD), FITC–anti-TCRβ (H57–597; BD), PE–anti-CXCR5 (2G8; BD), rabbit polyclonal anti-AID (H-80; Santa Cruz Biotechnology, Inc.), purified anti-FDC (FDC-M1; BD), purified anti-PNAd (MECA 79; BD), biotinylated anti–MAdCAM-1 (MECA-89; BD), biotinylated anti–VCAM-1 (429; BD), biotinylated peanut agglutinin (PNA; Vector Laboratories), rhodamine–UEA-1 (Vector Laboratories), Alexa Fluor 633–wheat germ agglutinin (Invitrogen), and FITC–NKM16-2-4 (Nochi et al., 2007). To visualize AID, FDC, MAdCAM-1, VCAM-1, PNAd, and PNA, FITC–anti–rabbit IgG (Santa Cruz Biotechnology, Inc.), FITC–anti–rat Ig κ chain (MRK-1; BD), FITC–anti–rat IgM (G53-238; BD), streptavidin-FITC (BD), and streptavidin-PE (eBioscience) were used as secondary antibodies or reagents. In some experiments, tissues were counterstained with DAPI (Sigma-Aldrich) to visualize the nucleus. *P. aeruginosa* PAO1 was detected with a rabbit polyclonal antibody specific for the bacterium (Abcam), followed by staining with FITC–anti–rabbit IgG (Santa Cruz Biotechnology, Inc.).

Ocular administration of bacteria. GFP-*Salmonella* (Jang et al., 2004) and *P. aeruginosa* PAO1 (Parks and Hobden, 2005) were administered as ocular antigens. After a 30-min administration of GFP-*Salmonella*, the mouse's ocular surface was washed with 100 μg/ml gentamycin. *P. aeruginosa* PAO1 is characterized by motility, biofilm formation, acyl-homoserine lactone production, and virulence in a mouse infection model (Parks and Hobden, 2005). These bacteria were cultured in Luria broth medium at 37°C for 18 h and used for ocular administration, as previously described (Jang et al., 2004). PAO1 was given twice with an interval of 1 wk (Hazlett et al., 2001).

Immunization and analysis of antigen-specific immune responses. Mice were ocularly immunized with 1 μg CT per eye (Sigma-Aldrich) in 5 μl PBS by eye drops three times at weekly intervals. Tissues or cells were collected from the heads of the ocularly immunized mice 7 d after the final immunization. To characterize CT-specific antibody responses, a CT-B–specific ELISPOT assay was used. In brief, 96-well plates (MultiScreen; Millipore) were coated with 2 μg/ml CT-B in 100 μl PBS (pH 7.4) per well for 16 h. The plates were washed three times with PBS and blocked with 100 μl of RPMI 1640 supplemented with 10% FCS for 30 min. After the blocking solution was discarded, 100 μl of cell suspension was applied to the well (tear duct, 10^4 cells/well; spleen, 10^6 cells/well). After incubation for 4 h, the plates were washed three times with PBS, followed by three washes with 0.1% Tween-PBS. The plates were incubated with horseradish peroxidase–conjugated anti–mouse IgA or IgG (1:1,000 dilution [vol/vol] in 0.1% Tween-PBS) for 16 h. After the plate had been washed with PBS six times, antibody-producing cells were visualized with AECB-500 and AECM-100 conjugate solutions (Moss, Inc.). Plates were incubated for 30 min and washed with water. The plates were allowed to dry, and spot pictures were taken with a microscope. To detect CT-B–specific T cells, a CT-B/I-A^b tetramer was prepared and used for flow cytometric analysis, as previously described (Chang et al., 2008).

Cell preparation and RT-PCR. $CD3^-CD4^+CD45^+$ cells were isolated from mucosa-associated tissues as previously described (Fukuyama et al., 2006). In some experiments, mononuclear cells were isolated from the TALT, NALT, and NPs of immunized mice by mechanical dissociation (Fukuyama et al., 2002). Total RNA was extracted for RT-PCR as previously described (Shikina et al., 2004). The sequences of primers used were as follows: *Id2*, (sense) 5′-TCTGAGCTTATGTCGAATGATAGC-3′ and (anti-sense) 5′-CACAGCATTCAGTAGGCTCGTGTC-3′; *Rorγt*, (sense) 5′-ACCTCCACTGCCAGCTGTGTGCTGTC-3′ and (anti-sense) 5′-TTGTTTCTGCACTTCTGCATGTAGACTGTCCC-3′; *Gapdh*, (sense) 5′-TGAACGGGAAGCTCACTGG-3′ and (anti-sense) 5′-TCCACCACCCTGTTGCTGTA-3′; *Aid*, (sense) 5′-GGCTGAGGTTAGGGTTCCATCTCAG-3′ and (anti-sense) 5′-GAGGGAGTCAAGAAAGTCACGCTGGA-3′; and *β-actin*, (sense) 5′-TGGAATCCTGTGGCATCCATGAAA-3′ and (anti-sense) 5′-TAAAACGCAGCTCAGTAACAGTCC-3′.

Electron microscopy analysis. Electron microscopy was performed as previously described (Jang et al., 2004). Head tissue containing the tear ducts was prepared and fixed in a solution containing 0.5% glutaraldehyde, 4% paraformaldehyde, and 0.1 M of sodium phosphate buffer (pH 7.6) on ice for 1 h. After washes with 4% sucrose in 0.1 M of phosphate buffer, the tissue was decalcified with 2.5% EDTA solution for 5 d. After three washes, the samples were fixed with 2% osmium tetraoxide on ice for 1 h and dehydrated with a series of ethanol gradients. For scanning electron microscopy, dehydrated tissues were freeze embedded in *t*-butyl alcohol and freeze dried, and then coated with osmium and observed under a scanning electron microscope (S-4200; Hitachi). For transmission electron microscopy, the tissues were embedded in Epon 812 resin mixture, and ultrathin (70-nm) sections were cut with an ultramicrotome (Reichert Ultracut N; Leica). The ultrathin sections were stained with 2% uranyl acetate in 70% ethanol for 5 min at room temperature and then in Reynold's lead for 5 min at room temperature. Sections were analyzed with a transmission electron microscope (H-7500; Hitachi).

Online supplemental material. Fig. S1 shows postnatal organogenesis of TALT on BALB/c mice. Fig. S2 shows development of TALT in B cell– or T cell–null mice and in TLR signaling–null conditions. Fig. S3 shows the lymphoid structure of TALT in mice lacking molecules related to lymphoid tissue genesis. Paraffinized sections were prepared from 8-wk-old mice and stained with the indicated antibodies (PNAd and B220) for confocal microscopy analysis. Arrows indicate PNAd-expressing HEVs. Fig. S4 shows the absence of MAdCAM-1 in TALT and NALT. TALT (A) and NALT (B) of 8-wk-old C57BL/6 mice were stained with DAPI and an anti–MAdCAM-1 antibody, and confocal microscopy analysis was performed. PPs of 10-d-old mice were analyzed as a positive control for anti–MAdCAM-1 antibody (C). Fig. S5 shows the independence of TALT genesis in TRANCE-Traf6 signaling. TALT of 2–3-wk-old *Trance*-deficient and *Traf6*, *Tcrb* double-deficient mice was analyzed histologically with hematoxylin and eosin (HE) staining. $Traf6^{+/-}$, $Tcrb^{-/-}$ mice were examined as a control. Online supplemental material is available at http://www.jem.org/cgi/content/full/jem.20091436/DC1.

We thank Dr. K. McGhee of the Medical College of Georgia for editorial help.

This work was supported by grants-in-aid from the Ministry of Education, Culture, Sports, Science, and Technology (MEXT), the Ministry of Health and Welfare of Japan and the Global Center of Excellence Program "Center of Education and Research for the Advanced Genome-Based Medicine For Personalized Medicine and the Control of Worldwide Infectious Diseases," and an "Academic Frontier" project for private universities matching-fund subsidy from MEXT. T. Nagatake, S. Fukuyama, and D.-Y. Kim were supported by research fellowships from the Japan Society for the Promotion of Science for Graduate Students, Young Scientists, and Foreign Researchers, respectively. A.M. Jetten was supported by the Intramural Research Program of the National Institute of Environmental Health Sciences (grant Z01-ES-101586).

The authors declare that they have no competing financial interests.

Submitted: 2 July 2009
Accepted: 16 September 2009

REFERENCES

Adachi, O., T. Kawai, K. Takeda, M. Matsumoto, H. Tsutsui, M. Sakagami, K. Nakanishi, and S. Akira. 1998a. Targeted disruption of the *MyD88* gene results in loss of IL-1- and IL-18-mediated function. *Immunity*. 9:143–150. doi:10.1016/S1074-7613(00)80596-8

Adachi, S., H. Yoshida, K. Honda, K. Maki, K. Saijo, K. Ikuta, T. Saito, and S.-I. Nishikawa. 1998b. Essential role of IL-7 receptor α in the formation of Peyer's patch anlage. *Int. Immunol.* 10:1–6. doi:10.1093/intimm/10.1.1

Allansmith, M.R., J. Radl, J.J. Haaijman, and J. Mestecky. 1985. Molecular forms of tear IgA and distribution of IgA subclasses in human lacrimal glands. *J. Allergy Clin. Immunol.* 76:569–576. doi:10.1016/0091-6749(85)90777-8

Ansel, K.M., V.N. Ngo, P.L. Hyman, S.A. Luther, R. Förster, J.D. Sedgwick, J.L. Browning, M. Lipp, and J.G. Cyster. 2000. A chemokine-driven positive feedback loop organizes lymphoid follicles. *Nature.* 406:309–314. doi:10.1038/35018581

Banks, T.A., B.T. Rouse, M.K. Kerley, P.J. Blair, V.L. Godfrey, N.A. Kuklin, D.M. Bouley, J. Thomas, S. Kanangat, and M.L. Mucenski. 1995. Lymphotoxin-α-deficient mice. Effects on secondary lymphoid organ development and humoral immune responsiveness. *J. Immunol.* 155:1685–1693.

Boos, M.D., Y. Yokota, G. Eberl, and B.L. Kee. 2007. Mature natural killer cell and lymphoid tissue–inducing cell development requires Id2-mediated suppression of E protein activity. *J. Exp. Med.* 204:1119–1130. doi:10.1084/jem.20061959

Browning, J.L., N. Allaire, A. Ngam-Ek, E. Notidis, J. Hunt, S. Perrin, and R.A. Fava. 2005. Lymphotoxin-β receptor signaling is required for the homeostatic control of HEV differentiation and function. *Immunity.* 23:539–550. doi:10.1016/j.immuni.2005.10.002

Cain, C., and T.E. Phillips. 2008. Developmental changes in conjunctiva-associated lymphoid tissue of the rabbit. *Invest. Ophthalmol. Vis. Sci.* 49:644–649. doi:10.1167/iovs.07-0856

Chang, S.-Y., H.-R. Cha, S. Uematsu, S. Akira, O. Igarashi, H. Kiyono, and M.-N. Kweon. 2008. Colonic patches direct the cross-talk between systemic compartments and large intestine independently of innate immunity. *J. Immunol.* 180:1609–1618.

Chodosh, J., R.E. Nordquist, and R.C. Kennedy. 1998. Comparative anatomy of mammalian conjunctival lymphoid tissue: a putative mucosal immune site. *Dev. Comp. Immunol.* 22:621–630. doi:10.1016/S0145-305X(98)00022-6

Dejardin, E., N.M. Droin, M. Delhase, E. Haas, Y. Cao, C. Makris, Z.-W. Li, M. Karin, C.F. Ware, and D.R. Green. 2002. The lymphotoxin-β receptor induces different patterns of gene expression via two NF-kappaB pathways. *Immunity.* 17:525–535. doi:10.1016/S1074-7613(02)00423-5

De Togni, P., J. Goellner, N.H. Ruddle, P.R. Streeter, A. Fick, S. Mariathasan, S.C. Smith, R. Carlson, L.P. Shornick, J. Strauss-Schoenberger, et al. 1994. Abnormal development of peripheral lymphoid organs in mice deficient in lymphotoxin. *Science.* 264:703–707. doi:10.1126/science.8171322

Eberl, G., and D.R. Littman. 2004. Thymic origin of intestinal alphabeta T cells revealed by fate mapping of RORgammat+ cells. *Science.* 305:248–251. doi:10.1126/science.1096472

Eberl, G., S. Marmon, M.J. Sunshine, P.D. Rennert, Y. Choi, and D.R. Littman. 2004. An essential function for the nuclear receptor RORgamma(t) in the generation of fetal lymphoid tissue inducer cells. *Nat. Immunol.* 5:64–73. doi:10.1038/ni1022

Ebisuno, Y., T. Tanaka, N. Kanemitsu, H. Kanda, K. Yamaguchi, T. Kaisho, S. Akira, and M. Miyasaka. 2003. Cutting edge: the B cell chemokine CXC chemokine ligand 13/B lymphocyte chemoattractant is expressed in the high endothelial venules of lymph nodes and Peyer's patches and affects B cell trafficking across high endothelial venules. *J. Immunol.* 171:1642–1646.

Fukuyama, S., T. Hiroi, Y. Yokota, P.D. Rennert, M. Yanagita, N. Kinoshita, S. Terawaki, T. Shikina, M. Yamamoto, Y. Kurono, and H. Kiyono. 2002. Initiation of NALT organogenesis is independent of the IL-7R, LTbetaR, and NIK signaling pathways but requires the Id2 gene and CD3(–)CD4(+)CD45(+) cells. *Immunity.* 17:31–40. doi:10.1016/S1074-7613(02)00339-4

Fukuyama, S., T. Nagatake, D.-Y. Kim, K. Takamura, E.J. Park, T. Kaisho, N. Tanaka, Y. Kurono, and H. Kiyono. 2006. Cutting edge: Uniqueness of lymphoid chemokine requirement for the initiation and maturation of nasopharynx-associated lymphoid tissue organogenesis. *J. Immunol.* 177:4276–4280.

Giuliano, E.A., C.P. Moore, and T.E. Phillips. 2002. Morphological evidence of M cells in healthy canine conjunctiva-associated lymphoid tissue. *Graefes Arch. Clin. Exp. Ophthalmol.* 240:220–226. doi:10.1007/s00417-002-0429-3

Gomes, J.A.P., V.K. Jindal, P.D. Gormley, and H.S. Dua. 1997. Phenotypic analysis of resident lymphoid cells in the conjunctiva and adnexal tissues of rat. *Exp. Eye Res.* 64:991–997. doi:10.1006/exer.1997.0297

Gupta, A., D. Monroy, Z. Ji, K. Yoshino, A. Huang, and S.C. Pflugfelder. 1996. Transforming growth factor beta-1 and beta-2 in human tear fluid. *Curr. Eye Res.* 15:605–614. doi:10.3109/02713689609008900

Hamada, H., T. Hiroi, Y. Nishiyama, H. Takahashi, Y. Masunaga, S. Hachimura, S. Kaminogawa, H. Takahashi-Iwanaga, T. Iwanaga, H. Kiyono, et al. 2002. Identification of multiple isolated lymphoid follicles on the antimesenteric wall of the mouse small intestine. *J. Immunol.* 168:57–64.

Harmsen, A., K. Kusser, L. Hartson, M. Tighe, M.J. Sunshine, J.D. Sedgwick, Y. Choi, D.R. Littman, and T.D. Randall. 2002. Cutting edge: organogenesis of nasal-associated lymphoid tissue (NALT) occurs independently of lymphotoxin-α (LT α) and retinoic acid receptor-related orphan receptor-γ, but the organization of NALT is LT α dependent. *J. Immunol.* 168:986–990.

Haynes, R.J., P.J. Tighe, and H.S. Dua. 1998. Innate defence of the eye by antimicrobial defensin peptides. *Lancet.* 352:451–452. doi:10.1016/S0140-6736(05)79185-6

Hazlett, L.D., S. McClellan, R. Barrett, and X. Rudner. 2001. B7/CD28 costimulation is critical in susceptibility to *Pseudomonas aeruginosa* corneal infection: a comparative study using monoclonal antibody blockade and CD28-deficient mice. *J. Immunol.* 166:1292–1299.

Honda, K., H. Nakano, H. Yoshida, S. Nishikawa, P. Rennert, K. Ikuta, M. Tamechika, K. Yamaguchi, T. Fukumoto, T. Chiba, and S.-I. Nishikawa. 2001. Molecular basis for hematopoietic/mesenchymal interaction during initiation of Peyer's patch organogenesis. *J. Exp. Med.* 193:621–630. doi:10.1084/jem.193.5.621

Hoshino, K., O. Takeuchi, T. Kawai, H. Sanjo, T. Ogawa, Y. Takeda, K. Takeda, and S. Akira. 1999. Cutting edge: Toll-like receptor 4 (TLR4)-deficient mice are hyporesponsive to lipopolysaccharide: evidence for TLR4 as the *Lps* gene product. *J. Immunol.* 162:3749–3752.

Jang, M.H., M.N. Kweon, K. Iwatani, M. Yamamoto, K. Terahara, C. Sasakawa, T. Suzuki, T. Nochi, Y. Yokota, P.D. Rennert, et al. 2004. Intestinal villous M cells: an antigen entry site in the mucosal epithelium. *Proc. Natl. Acad. Sci. USA.* 101:6110–6115. doi:10.1073/pnas.0400969101

Kanamori, Y., K. Ishimaru, M. Nanno, K. Maki, K. Ikuta, H. Nariuchi, and H. Ishikawa. 1996. Identification of novel lymphoid tissues in murine intestinal mucosa where clusters of c-kit$^+$ IL-7R$^+$ Thy1$^+$ lympho-hemopoietic progenitors develop. *J. Exp. Med.* 184:1449–1459. doi:10.1084/jem.184.4.1449

Kelsoe, G. 1996. Life and death in germinal centers (redux). *Immunity.* 4:107–111. doi:10.1016/S1074-7613(00)80675-5

Kijlstra, A. 1990. The role of lactoferrin in the nonspecific immune response on the ocular surface. *Reg. Immunol.* 3:193–197.

Kiyono, H., and S. Fukuyama. 2004. NALT- versus Peyer's-patch-mediated mucosal immunity. *Nat. Rev. Immunol.* 4:699–710. doi:10.1038/nri1439

Knop, N., and E. Knop. 2000. Conjunctiva-associated lymphoid tissue in the human eye. *Invest. Ophthalmol. Vis. Sci.* 41:1270–1279.

Knop, E., and N. Knop. 2001. Lacrimal drainage-associated lymphoid tissue (LDALT): a part of the human mucosal immune system. *Invest. Ophthalmol. Vis. Sci.* 42:566–574.

Knop, N., and E. Knop. 2005. Ultrastructural anatomy of CALT follicles in the rabbit reveals characteristics of M-cells, germinal centres and high endothelial venules. *J. Anat.* 207:409–426. doi:10.1111/j.1469-7580.2005.00470.x

Kong, Y.Y., H. Yoshida, I. Sarosi, H.-L. Tan, E. Timms, C. Capparelli, S. Morony, A.J. Oliveira-dos-Santos, G. Van, A. Itie, et al. 1999. OPGL is a key regulator of osteoclastogenesis, lymphocyte development and lymph-node organogenesis. *Nature.* 397:315–323. doi:10.1038/16852

Kurebayashi, S., E. Ueda, M. Sakaue, D.D. Patel, A. Medvedev, F. Zhang, and A.M. Jetten. 2000. Retinoid-related orphan receptor γ

(RORgamma) is essential for lymphoid organogenesis and controls apoptosis during thymopoiesis. *Proc. Natl. Acad. Sci. USA*. 97:10132–10137. doi:10.1073/pnas.97.18.10132

Liesegang, T.J. 1998. Bacterial and fungal keratitis. *In* The Cornea. H.E. Kaufman, B.A. Barron, M.B. McDonald, and S.R. Waltman, editors. Churchill Livingstone, New York. 217–270.

Luther, S.A., K.M. Ansel, and J.G. Cyster. 2003. Overlapping roles of CXCL13, interleukin 7 receptor α, and CCR7 ligands in lymph node development. *J. Exp. Med.* 197:1191–1198. doi:10.1084/jem.20021294

Mebius, R.E. 2003. Organogenesis of lymphoid tissues. *Nat. Rev. Immunol.* 3:292–303. doi:10.1038/nri1054

Mebius, R.E., P. Rennert, and I.L. Weissman. 1997. Developing lymph nodes collect CD4+CD3− LTbeta+ cells that can differentiate to APC, NK cells, and follicular cells but not T or B cells. *Immunity*. 7:493–504. doi:10.1016/S1074-7613(00)80371-4

Mestecky, J., R. Blumberg, H. Kiyono, and J.R. McGhee. 2003. Chapter 31. *In* Fundamental Immunology. Fifth edition. W.E. Paul, editor. Academic Press, San Diego. 965–1020.

Naito, A., S. Azuma, S. Tanaka, T. Miyazaki, S. Takaki, K. Takatsu, K. Nakao, K. Nakamura, M. Katsuki, T. Yamamoto, and J. Inoue. 1999. Severe osteopetrosis, defective interleukin-1 signalling and lymph node organogenesis in *TRAF6*-deficient mice. *Genes Cells*. 4:353–362. doi:10.1046/j.1365-2443.1999.00265.x

Naito, T., T. Shiohara, T. Hibi, M. Suematsu, and H. Ishikawa. 2008. ROR γ t is dispensable for the development of intestinal mucosal T cells. *Mucosal Immunol.* 1:198–207. doi:10.1038/mi.2008.4

Nakamura, Y., C. Sotozono, and S. Kinoshita. 1998. Inflammatory cytokines in normal human tears. *Curr. Eye Res.* 17:673–676. doi:10.1080/02713689808951242

Nakano, H., T. Tamura, T. Yoshimoto, H. Yagita, M. Miyasaka, E.C. Butcher, H. Nariuchi, T. Kakiuchi, and A. Matsuzawa. 1997. Genetic defect in T lymphocyte-specific homing into peripheral lymph nodes. *Eur. J. Immunol.* 27:215–221. doi:10.1002/eji.1830270132

Nakano, H., S. Mori, H. Yonekawa, H. Nariuchi, A. Matsuzawa, and T. Kakiuchi. 1998. A novel mutant gene involved in T-lymphocyte-specific homing into peripheral lymphoid organs on mouse chromosome 4. *Blood*. 91:2886–2895.

Nochi, T., Y. Yuki, A. Matsumura, M. Mejima, K. Terahara, D.-Y. Kim, S. Fukuyama, K. Iwatsuki-Horimoto, Y. Kawaoka, T. Kohda, et al. 2007. A novel M cell–specific carbohydrate-targeted mucosal vaccine effectively induces antigen-specific immune responses. *J. Exp. Med.* 204:2789–2796. doi:10.1084/jem.20070607

Parks, Q.M., and J.A. Hobden. 2005. Polyphosphate kinase 1 and the ocular virulence of *Pseudomonas aeruginosa*. *Invest. Ophthalmol. Vis. Sci.* 46:248–251. doi:10.1167/iovs.04-0340

Paulsen, F.P., J.I. Paulsen, A.B. Thale, and B.N. Tillmann. 2000. Mucosa-associated lymphoid tissue in human efferent tear ducts. *Virchows Arch.* 437:185–189. doi:10.1007/s004280000248

Paulsen, F.P., U. Schaudig, S. Maune, and A.B. Thale. 2003. Loss of tear duct-associated lymphoid tissue in association with the scarring of symptomatic dacryostenosis. *Ophthalmology*. 110:85–92. doi:10.1016/S0161-6420(02)01442-2

Peppard, J.V., and P.C. Montgomery. 1987. Studies on the origin and composition of IgA in rat tears. *Immunology*. 62:193–198.

Peschon, J.J., P.J. Morrissey, K.H. Grabstein, F.J. Ramsdell, E. Maraskovsky, B.C. Gliniak, L.S. Park, S.F. Ziegler, D.E. Williams, C.B. Ware, et al. 1994. Early lymphocyte expansion is severely impaired in interleukin 7 receptor–deficient mice. *J. Exp. Med.* 180:1955–1960. doi:10.1084/jem.180.5.1955

Rangel-Moreno, J., J. Moyron-Quiroz, K. Kusser, L. Hartson, H. Nakano, and T.D. Randall. 2005. Role of CXC chemokine ligand 13, CC chemokine ligand (CCL) 19, and CCL21 in the organization and function of nasal-associated lymphoid tissue. *J. Immunol.* 175:4904–4913.

Rangel-Moreno, J., J.E. Moyron-Quiroz, D.M. Carragher, K. Kusser, L. Hartson, A. Moquin, and T.D. Randall. 2009. Omental milky spots develop in the absence of lymphoid tissue-inducer cells and support B and T cell response to peritoneal antigens. *Immunity*. 30:731–743. doi:10.1016/j.immuni.2009.03.014

Rennert, P.D., D. James, F. Mackay, J.L. Browning, and P.S. Hochman. 1998. Lymph node genesis is induced by signaling through the lymphotoxin β receptor. *Immunity*. 9:71–79. doi:10.1016/S1074-7613(00)80589-0

Ridley Lathers, D.M., R.F. Gill, and P.C. Montgomery. 1998. Inductive pathways leading to rat tear IgA antibody responses. *Invest. Ophthalmol. Vis. Sci.* 39:1005–1011.

Saitoh-Inagawa, W., T. Hiroi, M. Yanagita, H. Iijima, E. Uchio, S. Ohno, K. Aoki, and H. Kiyono. 2000. Unique characteristics of lacrimal glands as a part of mucosal immune network: high frequency of IgA-committed B-1 cells and NK1.1+ alphabeta T cells. *Invest. Ophthalmol. Vis. Sci.* 41:138–144.

Shapiro-Shelef, M., and K. Calame. 2005. Regulation of plasma-cell development. *Nat. Rev. Immunol.* 5:230–242. doi:10.1038/nri1572

Shikina, T., T. Hiroi, K. Iwatani, M.H. Jang, S. Fukuyama, M. Tamura, T. Kubo, H. Ishikawa, and H. Kiyono. 2004. IgA class switch occurs in the organized nasopharynx- and gut-associated lymphoid tissue, but not in the diffuse lamina propria of airways and gut. *J. Immunol.* 172:6259–6264.

Shinkura, R., K. Kitada, F. Matsuda, K. Tashiro, K. Ikuta, M. Suzuki, K. Kogishi, T. Serikawa, and T. Honjo. 1999. Alymphoplasia is caused by a point mutation in the mouse gene encoding Nf-κ b-inducing kinase. *Nat. Genet.* 22:74–77. doi:10.1038/8780

Stein-Streilein, J., and A.W. Taylor. 2007. An eye's view of T regulatory cells. *J. Leukoc. Biol.* 81:593–598. doi:10.1189/jlb.0606383

Sullivan, D.A., and M.R. Allansmith. 1984. Source of IgA in tears of rats. *Immunology*. 53:791–799.

Sun, Z., D. Unutmaz, Y.R. Zou, M.J. Sunshine, A. Pierani, S. Brenner-Morton, R.E. Mebius, and D.R. Littman. 2000. Requirement for RORgamma in thymocyte survival and lymphoid organ development. *Science*. 288:2369–2373. doi:10.1126/science.288.5475.2369

Suzuki, K., T. Oida, H. Hamada, O. Hitotsumatsu, M. Watanabe, T. Hibi, H. Yamamoto, E. Kubota, S. Kaminogawa, and H. Ishikawa. 2000. Gut cryptopatches: direct evidence of extrathymic anatomical sites for intestinal T lymphopoiesis. *Immunity*. 13:691–702. doi:10.1016/S1074-7613(00)00068-6

Takeuchi, O., K. Hoshino, T. Kawai, H. Sanjo, H. Takada, T. Ogawa, K. Takeda, and S. Akira. 1999. Differential roles of TLR2 and TLR4 in recognition of gram-negative and gram-positive bacterial cell wall components. *Immunity*. 11:443–451. doi:10.1016/S1074-7613(00)80119-3

Taylor, R.T., A. Lügering, K.A. Newell, and I.R. Williams. 2004. Intestinal cryptopatch formation in mice requires lymphotoxin α and the lymphotoxin β receptor. *J. Immunol.* 173:7183–7189.

Tsuji, M., K. Suzuki, H. Kitamura, M. Maruya, K. Kinoshita, I.I. Ivanov, K. Itoh, D.R. Littman, and S. Fagarasan. 2008. Requirement for lymphoid tissue-inducer cells in isolated follicle formation and T cell-independent immunoglobulin A generation in the gut. *Immunity*. 29:261–271. doi:10.1016/j.immuni.2008.05.014

Uchio, E., S.Y. Ono, Z. Ikezawa, and S. Ohno. 2000. Tear levels of interferon-gamma, interleukin (IL)-2, IL-4 and IL-5 in patients with vernal keratoconjunctivitis, atopic keratoconjunctivitis and allergic conjunctivitis. *Clin. Exp. Allergy*. 30:103–109. doi:10.1046/j.1365-2222.2000.00699.x

Yokota, Y., A. Mansouri, S. Mori, S. Sugawara, S. Adachi, S. Nishikawa, and P. Gruss. 1999. Development of peripheral lymphoid organs and natural killer cells depends on the helix-loop-helix inhibitor Id2. *Nature*. 397:702–706. doi:10.1038/17812